Polymer 50 (2009) 1403–1413

Contents lists available at ScienceDirect

Polymer

journal homepage: www.elsevier.com/locate/polymer

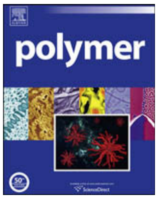

Variation in acid moiety of polybenzimidazoles: Investigation of physico-chemical properties towards their applicability as proton exchange and gas separation membrane materials

S.C. Kumbharkar, Md. Nazrul Islam, R.A. Potrekar, U.K. Kharul*

Polymer Science and Engineering Division, National Chemical Laboratory, Dr. Homi Bhabha Road, Pune 411008, Maharashtra, India

ARTICLE INFO

Article history:
Received 14 August 2008
Received in revised form
3 January 2009
Accepted 20 January 2009
Available online 24 January 2009

Keywords:
Polybenzimidazole
Proton exchange membrane
Gas permeability

ABSTRACT

A series of polybenzimidazoles (PBIs) were prepared from 3,3′-diaminobenzidine (DAB) and substituted aromatic dicarboxylic acids. Effects of added polarity, bulk and isomerism in the dicarboxylic acid moiety on the properties of formed aromatic polybenzimidazoles were investigated. Solution polycondensation procedure was optimized for individual case of PBI synthesis in order to obtain inherent viscosity of ≥1 dL/g. Analysis of physical properties, water uptake, acid doping (H_3PO_4 and H_2SO_4) and gas permeability was performed. All these PBIs exhibited high thermal stability, good solvent solubility and amorphous nature. The uptake of H_3PO_4 varied from 9 to 20.1 moles per repeat unit (mol/RU), H_2SO_4 uptake varied from 3.39 to 3.81 mol/RU, while water uptake varied from 1.8 to 3.6 mol/RU of PBI. The dibromoterephthalic acid and *tert*-butylisophthalic acid based PBI showed the highest H_3PO_4 uptake in the series, while *tert*-butylisophthalic acid based PBI exhibited the highest water uptake. Acid uptake was correlated with swelling of the PBI matrix, while density estimation of H_3PO_4-doped PBI by He gas expansion method could be correlated to the physical state of PBI. 5-*tert*-Butylisophthalic acid and 4,4′-(hexafluoroisopropylidene)bis(benzoic acid) based PBI exhibited higher H_2 and O_2 permeability than other PBIs. The ideal gas selectivity for O_2/H_2 was considerably higher for most of the PBIs than conventional gas separation membrane materials. These analyses suggested that some of these PBIs have a potential to be used as a PEM or gas separation membrane material.

1. Introduction

Polybenzimidazole (PBI) is one of the classes of heteroaromatic polymers known for many years following the early work of Vogel and Marvel [1]. One of the members of this family, commonly known as PBI (designated as PBI-I in this work) based on 3,3′-diaminobenzidine and isophthalic acid is gaining increasing importance as the proton exchange membrane (PEM) material. It has remarkable thermal stability, mechanical property, chemical resistance, fiber forming property, adhesion property, etc. Fuel cell based on its membrane can be operated up to 200 °C [2,3], has high CO tolerance [2,3], low fuel crossover [3,4], almost zero osmotic drag coefficient [4] and proton conductivity comparable to Nafion membrane [2–4]. This highly basic material is characterized by high density [5,6], high T_g [6], H_3PO_4 uptake of ∼14 moles per repeat unit (mol/RU) and 3.4–3.6 mol/RU of water sorption [7]. Applications of PBI in fiber and fabrics [8], as a membrane material [9–12], structural adhesives [13], hydrogen sensor [14], blends [15,16], composites with other polymers for various applications like microcellular foam [17], as a catalyst support in epoxidation of alkenes [18], nanofiber by electrospinning [19], etc. are documented. Owing to high thermal stability [1,20,21,26], PBI finds application in aerospace industry [22]. One of its important drawbacks includes limited solvent solubility [23,24]. It is soluble only in *N*,*N*-dimethylacetamide, dimethylsulphoxide and *N*-methylpyrrolidinone [25]. Various structural modifications have been attempted to improve its solubility. These attempts include introduction of isopropylidene and oxymethylene groups [26], methyl on the aromatic ring [27], methylene [24], cardo fluorene groups [28], nitro [23], bridge-oxygen [29], sulfone linkage [30], methylsiloxane [31,32], silane [33], hexafluoroisopropylidene [34], etc.

In the present work, a systematic variation in PBI family based on a common tetramine: 3,3′-diaminobenzidine (DAB) and different aromatic dicarboxylic acids is investigated. Isophthalic acid and terephthalic acid based PBIs were synthesized to investigate effects of substitution site (*meta* versus *para* substitution), 5-*tert*-butyl isophthalic acid and 4,4′-(hexafluoroisopropylidene)bis(benzoic acid) based PBIs were prepared to investigate effects of bulky

---

* Corresponding author. Tel.: +91 20 25902180; fax: +91 20 25902618.
E-mail address: uk.kharul@ncl.res.in (U.K. Kharul).

0032-3861/$ – see front matter © 2009 Elsevier Ltd. All rights reserved.
doi:10.1016/j.polymer.2009.01.043

groups; while 2,6-pyridinedicarboxylic acid, 2-bromoterephthalic acid and 2,6-dibromoterephthalic acid based PBIs were synthesized in order to investigate effects of increased polarity. Effects of variations by these substitutions on physical properties, H_3PO_4, H_2SO_4 and water uptake and gas permeability (H_2, O_2) of resulting PBIs shed a light on their applicability as proton exchange membranes for fuel cell and as gas separation membrane materials.

2. Experimental

2.1. Materials and monomers

3,3′-Diaminobenzidine (DAB), isophthalic acid (IPA), terephthalic acid (TPA), 4,4′-(hexafluoroisopropylidene)bis(benzoic acid) (HFA), 5-*tert*-butylisophthalic acid (BuI), 2-bromoterephthalic acid (BrTPA), 2,5-dibromoterephthalic acid (DBrTPA) and 2,6-pyridinedicarboxylic acid (PyA) were procured from Aldrich chemicals. Polyphosphoric acid (PPA) was procured from Lancaster, *N*,*N*-dimethylacetamide (DMAc) and concentrated H_2SO_4 (98%) were procured from Merck. Phosphoric acid (88%) was procured from Qualigens. All these materials were used without further purification. The chemical structures of aromatic dicarboxylic acids used in this work along with polymer abbreviations used are shown in Table 1. Pure gases used (H_2 and O_2) had a minimum purity of 99.9% and were procured from Inox.

2.2. Polymer synthesis

Polybenzimidazoles were synthesized by solution polycondensation method using PPA, which acts as a solvent as well as condensation agent [25,34]. Typically, a three-necked flask equipped with a mechanical stirrer, N_2 inlet and $CaCl_2$ drying tube was charged with 60 g of PPA, 2 g (0.0093 mol) of DAB and temperature was elevated to 100 °C. After complete dissolution, 0.0093 mol of dicarboxylic acid was added; temperature was slowly raised to 170 °C and maintained for 5 h under constant flow of nitrogen. The temperature was further raised to 200 °C and maintained for certain duration, depending upon the dicarboxylic acid used (Table 1). After completion of the reaction, temperature was lowered to ∼90 °C and the highly viscous reaction mixture was poured on to the stirred water. The precipitated polymer was crushed and thoroughly washed with water till it was neutral to pH. The polymer was then kept overnight in 10% aqueous Na_2CO_3, washed with water until neutral to pH and soaked in acetone for 16 h to extract water. The dried polymer (100 °C, 3 days) was further purified by dissolving in DMAc, removing undissolved material, if any, by centrifugation at 3000 rpm for 3 h and

Table 1
Synthesis details of polybenzimidazoles based on 3,3′-diaminobenzidine (DAB).

Polymer abbreviation	Dicarboxylic acid, HOOC–R–COOH		Reaction time at 200 °C (h)	η_{inh}[a] (dL/g)	Yield (%)
	Name of the acid	Chemical structure of R			
PBI-I	Isophthalic acid (IPA)	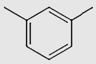	12	1.4	99
PBI-T	Terephthalic acid (TPA)	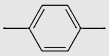	2	1.8	99
PBI–BuI	5-*tert*-Butylisophthalic acid (BuI)	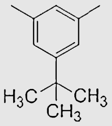	12	1.3	97
PBI–HFA	3,3′-(Hexafluoroisopropylidene)bis(benzoic acid) (HFA)	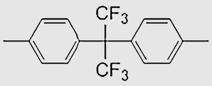	6	1.5	89
PBI–BrT	2-Bromoterephthalic acid (BrTPA)	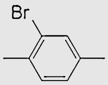	2	1.3	91
PBI–DBrT	2,5-Dibromoterephthalic acid (DBrTPA)	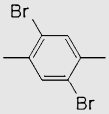	1	1.3	98
PBI–2,6Py	2,6-Pyridinedicarboxylic acid (PyA)	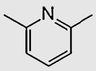	12	0.9	95

[a] Inherent viscosity using 0.2 g/dL solution in conc. H_2SO_4 at 35 °C.

reprecipitation on to the stirred water. The polymer was finally dried at 60 °C for 24 h and then in vacuum oven at 100 °C for 3 days.

2.3. Preparation of dense membrane

Dense membranes were prepared by solution casting method under identical conditions using 3% (w/v) polymer solution in DMAc; prepared while stirring at 80 °C for 14–18 h under dry atmosphere. The solution after centrifugation at 3000 rpm (to remove undissolved particles, if any) was poured on to the flat glass surface and heated at 80 °C for ~18 h under inert atmosphere. Formed film was peeled off and soaked in water at 60 °C for 3 days in order to remove traces of DMAc. Such films were finally dried in vacuum oven at 100 °C for a week and used for subsequent analyses.

2.4. Characterizations

The solubility in various solvents was evaluated with 1% PBI solution (w/v) as a criterion for solubility. The vacuum dried polymer was stirred in respective solvent at ambient temperature for 24 h and if required, heated to reflux (in the case of organic solvents) or at 120 °C (in the case of H_3PO_4) for 10–16 h. The observations are given in Table 2. The inherent viscosity (Table 1) was determined using Ubbelohde viscometer with 0.2 g/dL polymer concentration in 98% H_2SO_4 at 35 °C. FT-IR spectra of polymers in the thin film form were recorded on a Perkin Elmer-16-PC FT-IR spectrophotometer and are given in Fig. 1. ^{1}H NMR spectra were recorded on Bruker AC-200 using DMSO-d_6 as the solvent and are given in Fig. 2. The wide angle X-ray diffraction (WAXD) spectra of polymers in film form (~40 μm thick) were recorded using Rigaku X-ray diffractometer (D-max 2500) with Cu-Kα radiation in 2θ range of 5–40° and are shown in Fig. 3. The average d-spacing (d_{sp}) for the amorphous peak maxima was calculated using Bragg's equation (Table 3). The reproducibility of the d_{sp} measurement was ±0.04 Å. The thermogravimetric analysis (TGA) using ~40 μm thick film sample was performed on Perkin Elmer TGA-7 under N_2 atmosphere with the heating rate of 10 °C/min (Fig. 4). The density measurement using ~100 μm thick films was carried out at 35 °C by floatation method using mixtures of cyclohexanone with tetrachloroethane/iodomethane [10]. The measurements were repeated at least six times and the variation was found to be ±0.006 g/cm^3. Based on the density determinations, fractional free volume (v_f) and solubility parameter (δ) were calculated by the group contribution method [35] using following equations.

$$v_f = \frac{V_{sp} - V_w}{V_{sp}} \tag{1}$$

where, V_{sp} = specific volume and V_w = van der Waal's volume.

Table 2
Solubility of polybenzimidazoles in solvents of interest.

Polymer	DMAc	NMP	DMF	DMSO	Pyridine	HCOOH	CH_3COOH	H_2SO_4	H_3PO_4
PBI-I	++	++	++	++	−	+	±	++	±
PBI–BuI	++	++	++	++	±	++	−	++	+
PBI–HFA	++	++	++	++	++	++	−	++	−
PBI-T	+	±	±	±	−	±	±	++	±
PBI–DBrT	+	++	++	++	−	++	−	++	++
PBI–BrT	++	++	++	++	−	++	−	++	++
PBI–2,6Py	++	++	++	+	−	±	−	++	±

++: Soluble at ambient temperature.
+: Soluble at reflux temperature (120 °C in case of H_3PO_4).
±: Partially soluble or swelling after heating at reflux temperature in organic solvents, 120 °C in case of H_3PO_4.
−: Insoluble even after heating.

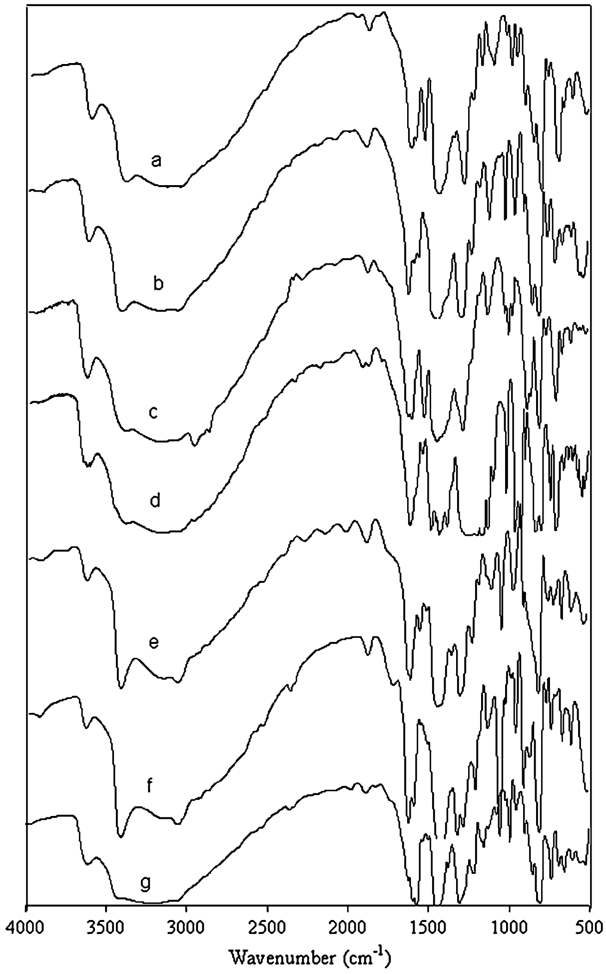

Fig. 1. FT-IR spectra of polybenzimidazoles (a: PBI-I, b: PBI-T, c: PBI–BuI, d: PBI–HFA, e: PBI–BrT, f: PBI–DBrT, g: PBI–2,6Py).

$$\delta = [E_{coh}/V]^{1/2} \tag{2}$$

where E_{coh} = cohesive energy of the polymer and V = molar volume of the polymer

2.5. Acid doping and water sorption

Membrane samples of 4 × 4 cm^2 (~60 μm thick) were dipped in water, H_3PO_4 and H_2SO_4 solution of various concentrations. The dip time required to achieve maximum possible doping was initially determined by keeping the PBI-I membrane in the phosphoric acid (16.2 M) and sulphuric acid (12 M) solution individually for various time intervals as shown in Fig. 5. The doping analyses for other PBIs with both the acid solutions of different concentrations were done by immersing membrane samples for 3 days into it, followed by vacuum drying at 100 °C for 3 days. The acid sorbed as a function of its concentration was determined gravimetrically and plotted in Figs. 6 and 7. The maximum amount of acid sorbed is given in Table 4, as an intrinsic property of that PBI. Water sorbed along with the acid (H_3PO_4 and H_2SO_4) was removed by vacuum drying at 100 °C for 3 days. This quantity of water estimated gravimetrically for various acid bath concentrations for different PBIs is plotted in Fig. 8. The maximum amount of water sorption in all the virgin PBIs was also determined gravimetrically by immersing vacuum dried membrane samples in water at 35 °C for 3 days. The acid/water sorption was determined with 6 samples

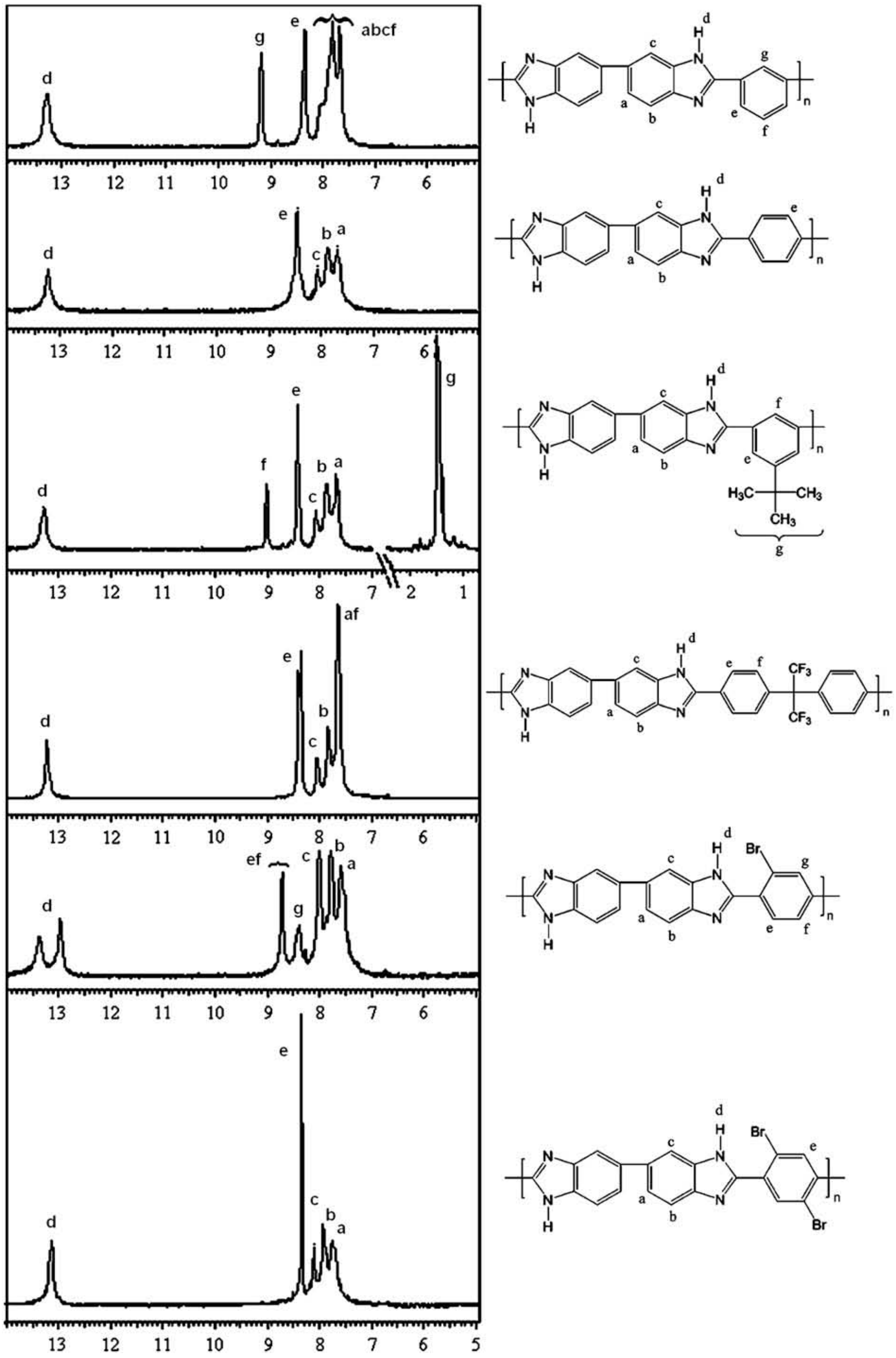

Fig. 2. ^{1}H NMR spectra of polybenzimidazoles (a: PBI-I, b: PBI-T, c: PBI–BuI, d: PBI–HFA, e: PBI–BrT, f: PBI–DBrT).

and data averaged. The percent sorption was calculated using following equation (3) and is given in Table 4.

$$\%\text{Sorption} = \frac{W_f - W_i}{W_i} \times 100 \tag{3}$$

where, W_f = weight of the membrane after sorption and W_i = initial weight of the vacuum dried membrane.

2.6. Measurement of volume of PBI doped with H_3PO_4

Volume of the H_3PO_4-doped PBI-I samples was determined by He gas expansion method [36]. The gas sorption equipment used for this purpose is described elsewhere [37]. The method assumes that a negligible amount of He is sorbed into the polymer over the time of exposure. This was confirmed by the absence of any observable pressure decay following the He expansion in chamber containing the PBI-I sample. The volume thus obtained was used to calculate density and plotted in Fig. 10 as a function of acid doping.

2.7. Gas permeability

Membrane samples of 10 cm diameter and 25–30 μm thickness were used for determining pure gas permeability of H_2 and O_2 by variable volume method [38] with upstream gas pressure of 300 psi

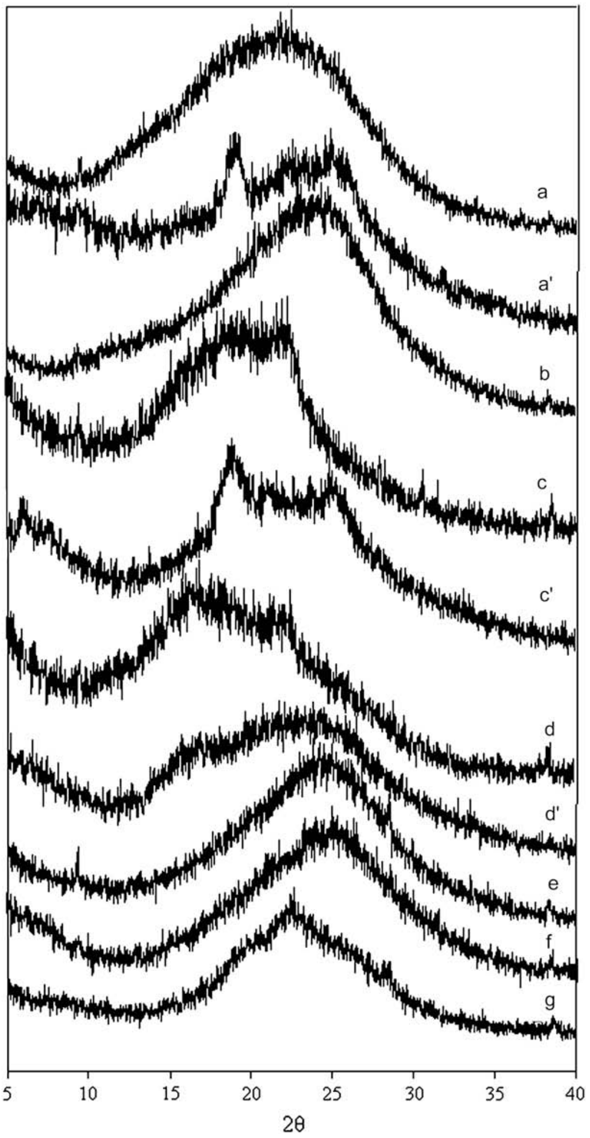

Fig. 3. Wide angle X-ray diffraction spectra of polybenzimidazoles (a: PBI-I, a′: H_3PO_4-doped PBI-I, b: PBI-T, c: PBI–BuI, c′: H_3PO_4-doped PBI–BuI, d: PBI–HFA, d′: H_3PO_4-doped PBI–HFA, e: PBI–BrT, f: PBI–DBrT, g: PBI–2,6Py).

Table 3
Physical properties of polybenzimidazoles.

Polymer	d_{sp}[a] (Å)	ρ[b] (g/cm^3)	v_f[c] (cm^3 cm^{-3})	δ[d] (cal cm^{-3})$^{1/2}$	TGA analysis		
					T_{wl}[e]	IDT[f] (°C)	T_{900}[g] (wt%)
PBI-I	4.05	1.331	0.3096	10.50	147	600	67
PBI-T	3.70	1.353	0.2982	10.59	179	620	82
PBI–BuI	4.69, 4.04	1.193	0.3393	9.63	136	525	65
PBI–HFA	5.37, 4.05	1.371	0.3605	9.19	128	535	61
PBI–BrT	3.70	1.553	0.3104	10.65	143	400	56
PBI–DBrT	3.63	1.717	0.3223	10.68	163	440	55
PBI–2,6Py	3.96	1.340	0.3226	10.57	187	600	78

[a] d-Spacing obtained from wide angle X-ray diffraction spectra.

[b] Density measured at 35 °C by floatation method.

[c] Fractional free volume ($v_f = 1 - V_w/V_{sp}$) calculated using group additivity method [35].

[d] Hildebrand solubility parameter estimated using Fedor's method [35].

[e] Temperature at which initial water loss occurred.

[f] Initial decomposition temperature.

[g] Char yield at 900 °C.

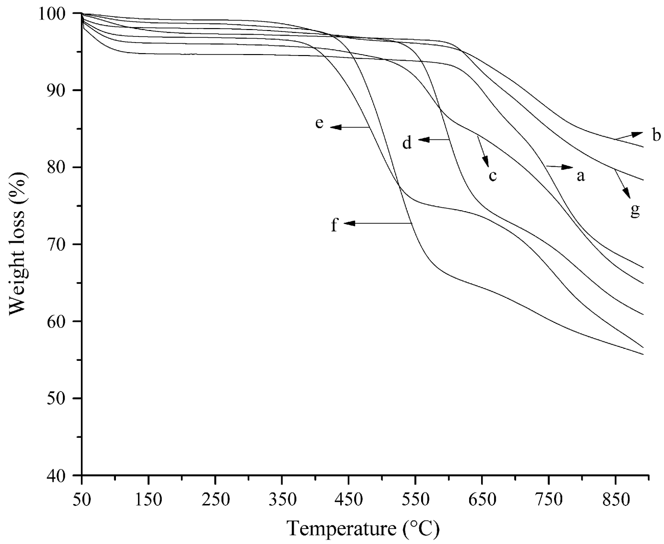

Fig. 4. TGA spectra of polybenzimidazoles (a: PBI-I, b: PBI-T, c: PBI–BuI, d: PBI–HFA, e: PBI–BrT, f: PBI–DBrT, g: PBI–2,6Py).

at 35 °C; while maintaining the permeate side at the ambient pressure. The permeability was determined using equation (4).

$$P = \frac{Nl}{p_2 - p_1} \tag{4}$$

where P, the permeability coefficient is expressed in Barrer, p_2 is the feed side pressure (cm Hg) and p_1 is the permeate side pressure (cm Hg), l is the membrane thickness (cm) and N is the steady-state penetrant flux (cm^3/s). The permeability measurements were repeated for 6 membrane samples prepared under identical conditions and the data averaged as given in Table 5. Variation in the permeability measurement was up to ±15% for both the gases.

3. Results and discussion

3.1. Polymer synthesis

The time of reaction at 200 °C was optimized for individual cases of PBI synthesis to achieve high enough inherent viscosity (~1 dL/g, Table 1). Reactions with 1,3-substituted dicarboxylic acids (isophthalic, 5-*tert*-butylisophthalic and 2,6-pyridinedicarboxylic acid) took almost 12 h at 200 °C. This time was drastically reduced

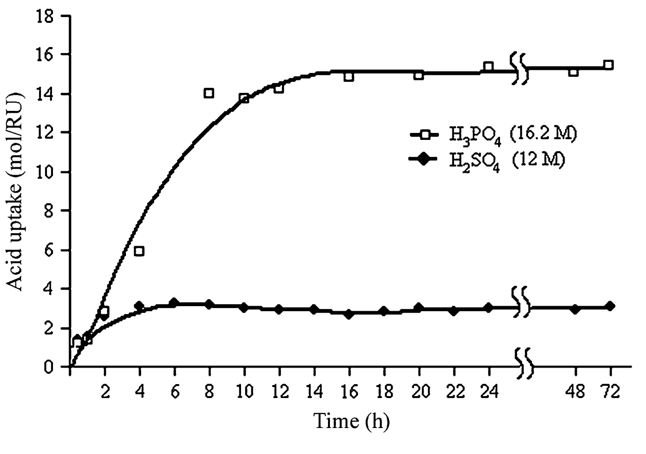

Fig. 5. H_3PO_4 (16.2 M) and H_2SO_4 (12 M) uptake in PBI-I with time.

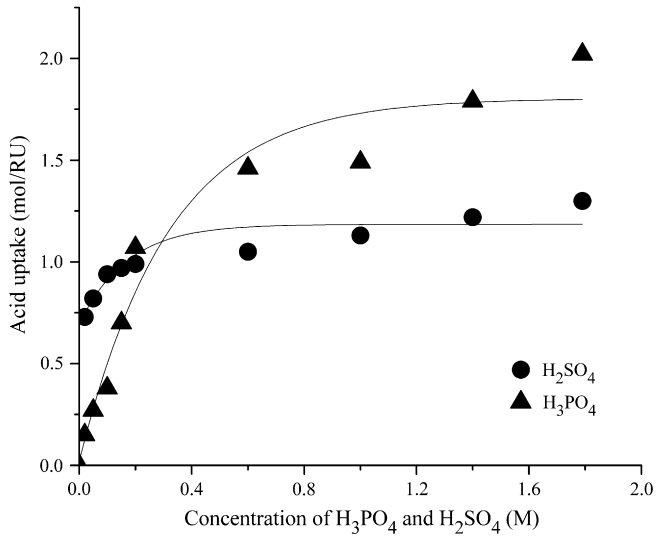

Fig. 6. Acid uptake in PBI-I at lower bath concentrations.

Table 4
Acid and water uptake by polybenzimidazoles.

Polymer	Water uptake		H_3PO_4 uptake[a]		Water uptake along with H_3PO_4		H_2SO_4 uptake[b]		Water uptake along with H_2SO_4	
	wt%	mol/RU	wt%	mol/RU	wt%	mol/RU	wt%	mol/RU	wt%	mol/RU
PBI-I	20.4	3.5	493	15.1	72	12.3	108	3.39	42.9	7.3
PBI-T	21.3	3.6	332	10.4	83.3	14.3	–	–	–	–
PBI-BuI	12.3	2.5	526	20	213	40.1	94.7	3.52	47.8	9.7
PBI-HFA	5.9	1.8	167	9	35.7	10.6	71.4	3.81	34.6	10
PBI-BrT	12.2	2.6	351	13.9	86	18.5	–	–	–	–
PBI-DBrT	8.5	2.2	430	20.1	57.5	14.9	–	–	–	–
PBI-2,6Py	17.6	3.0	579	18.3	172	29.5	120.7	3.79	53.4	9.1

[a] At H_3PO_4 bath concentration of 16.2 mol/L, except for PBI-BrT and PBI-DBrT, wherein, the acid bath concentration was 14.3 mol/L.
[b] At H_2SO_4 bath concentration of 12 mol/L.

when 1,4-substituted dicarboxylic acids (terephthalic, 2-bromoterephthalic and 2,5-dibromoterephthalic acid) were used. The difference in reactivity of these acids could be attributed to the substitution type. In latter cases, *para* (1,4-) substitution of –COOH groups leading to -I effect could be responsible for enhanced reactivity by nucleophilic substitution than for the former cases with *meta* (1,3-) substitution. Similar observations were reported by Iwakura et al. [25], wherein, the polycondensation reaction of terephthalic acid derivatives with 3,3′-diaminobenzidine tetrahydrochloride proceeded faster than that in the case of isophthalic acid derivatives. Vogel and Marvel [1] have also reported lesser reaction time for synthesizing PBI-T than for PBI-I by melt condensation using diphenyl ester of respective acids under similar temperature conditions. The reaction time required for DBrTPA was almost half than that for the TPA. The presence of an electron withdrawing bromine on the acid moiety could be responsible for this enhanced reactivity. The reaction period for HFA was 6 h, indicating electron withdrawing nature of hexafluoroisopropylidene group enhanced the rate of reaction, than that of isophthalic acid case. Choi et al. [39] have reported that the inductive effect of the electronegative fluorine would enhance the acid strength of HFA, leading to the higher reactivity of benzoyl group.

3.2. Physical properties

3.2.1. Solubility and spectral characterizations

The solvent solubility of these PBIs was evaluated with 1% w/v polymer concentration as a criterion and the results are summarized

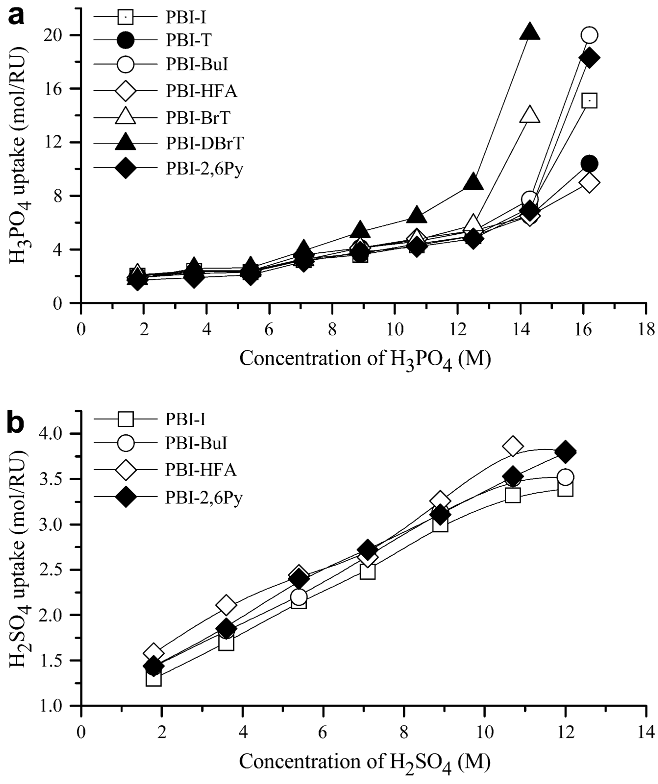

Fig. 7. Sorption of (a) H_3PO_4 and (b) H_2SO_4 in different polybenzimidazoles at various concentrations.

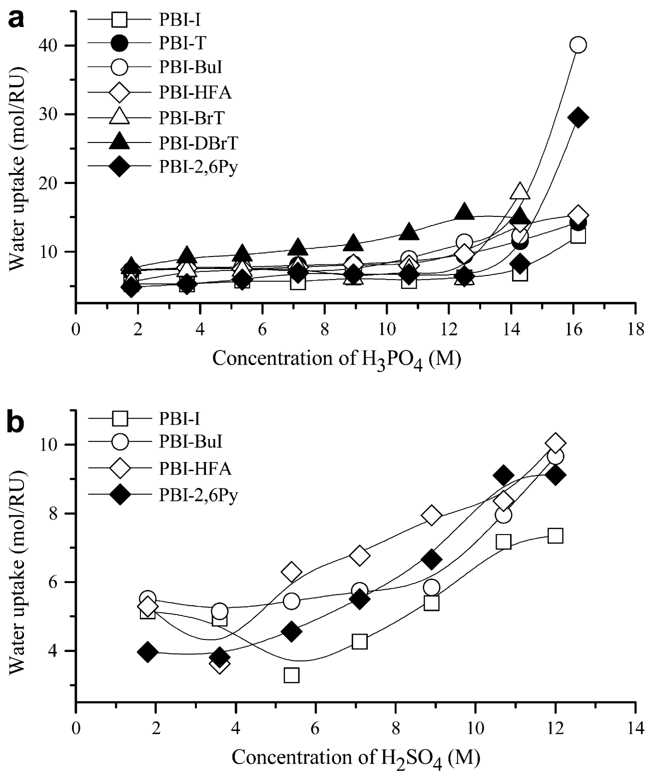

Fig. 8. Water uptake for different polybenzimidazoles along with (a) H_3PO_4 sorption and (b) H_2SO_4 sorption.

Table 5
Gas permeability (P)[a] and selectivity (α)[b] of polybenzimidazoles.

Polymer	$P(H_2)$	$P(O_2)$	$\alpha(H_2/O_2)$
Doped membranes			
PBI-I	1.27	0.31	4.1
PBI–BuI	0.72	0.15	4.8
PBI–HFA	1.09	0.13	8.4
Undoped membranes			
PBI-I	0.63	0.015	42
PBI-T	0.16	0.004	55
PBI–BuI	10.66	0.42	25.4
PBI–HFA[c]	12.15	0.60	20.1
PBI–BrT	0.38	0.006	60
PBI–DBrT	1.89	0.07	28
PBI–2,6Py	1.38	0.045	31
Polyarylate[d]	13.4	1.3	10.3
Polysulphone[e]	14	1.4	10

[a] Pure gas permeability in Barrer (1 Barrer = 10^{-10} cm^3 (STP) cm Hg^{-1} cm^{-1} s^{-1}).

[b] Ratio of pure gas permeability.

[c] From Ref. [10].

[d] From Ref. [47].

[e] From Ref. [45].

in Table 2. All polymers were soluble in conc. H_2SO_4. Nature of the dicarboxylic acid used for synthesizing PBI had its own effect on the solubility. Presence of the bulky (*tert*-butyl, hexafluoroisopropylidene) or polar (–Br) group on dicarboxylic acid moiety of PBI enhanced the solvent solubility. Except for PBI-T, all other PBIs were soluble in DMAc, NMP, DMF and DMSO at 1% concentration. Higher concentrations needed heating at 80–130 °C for 14–18 h. This duration was reduced to 2–4 h, if reflux conditions were used. PBI-T could be dissolved in DMAc only under heating. Lower solubility of PBI-T than that of PBI-I was reported by Vogel and Marvel [1] and Iwakura et al. [25]; which was attributed to the polymer chain rigidity, symmetry and intermolecular attraction. An introduction of *tert*-butyl group in PBI–BuI, hexafluoroisopropylidene group in PBI–HFA, bromine in PBI–BrT and PBI–DBrT offered solubility also in formic acid (85%) at ambient temperature and within a short time of an hour. On the other hand, PBI-I needed prolonged stirring for 12 h under reflux condition. PBI-T and PBI–2,6Py were partially soluble in formic acid at reflux temperature for 24 h. PBI–HFA was found to be soluble in pyridine also. This polymer was shown to possess attractive gas permeation properties [10]. Its solubility in pyridine and formic acid (which are volatile and water miscible) can be useful in transforming this material into required membrane type (thin film composite or asymmetric membranes) for gas separation and other membrane applications. Improved solubility of PBI–HFA in organic solvents and in acids is reported [34]. Brominated PBIs were soluble in 16.2 M H_3PO_4. Thus, their doping analysis was performed only up to 14.3 M of H_3PO_4. An introduction of alkyl group like methyl [27] and polar group like nitro [23] on PBI backbone is known to increase solubility. All present PBIs were insoluble in chloroform, dichloroethane, tetrachloroethane, 1,4-dioxane and tetrahydrofuran.

FT-IR spectra of these polymers are given in Fig. 1. The benzimidazole ring was characterized by the absorption at 1430, 1600, and 1620 cm^{-1} [40,41]. These peaks were common in all PBIs investigated. The region 1500–1650 cm^{-1} is the characteristic of benzimidazoles. These bands are derived from C=C and C=N stretching as well as ring modes, which are characteristic of conjugation between benzene and the imidazole rings [40,41]. The strong band at ~3145 cm^{-1} was ascribed to the hydrogen bonding of the type $N{-}H\cdots N$, while the peak at ~3410 cm^{-1} was due to the free non-hydrogen bonded N–H stretching. The peak around 3050 cm^{-1} was attributed to stretching of the aromatic C–H bond. The peak at 2862 cm^{-1} in the IR spectrum of PBI–BuI could be ascribed to the presence of the *tert*-butyl group on the acid moiety. In case of PBI–HFA, the broad band at 1134–1294 cm^{-1} could be attributed to the C–F stretching vibrations [39]. For all PBIs, the peak at 3598–3628 cm^{-1} could be attributed to the O–H stretching of absorbed water. Such peak was also observed by Brooks et al. [42] and Li et al. [43] at 3620 cm^{-1} and it was said to be removed by heating at 120 °C.

Fig. 2 shows the ^{1}H NMR signal assignments for present polybenzimidazoles. In all these PBIs, the peak due to hydrogen of imidazole proton was observed as a singlet at δ 13.1–13.3, except for PBI–BrT, wherein it appeared as a doublet at δ 13.0–13.3. Aromatic protons appeared between δ 7.5 and 9.2. The protons due to $-CH_3$ group in PBI–BuI appeared at δ 1.4 as a singlet. The ^{1}H NMR spectra of PBI–2,6Py could not be recorded due to its insolubility in DMSO-d_6 at ambient temperature.

WAXD analysis of undoped PBIs indicated that all of them are amorphous in nature (Fig. 3). The d-spacing (d_{sp}) corresponding to the amorphous peak maxima in WAXD spectra is given in Table 3. It could be seen that PBIs, in general, have much lower d_{sp} than that of common polymers like polysulfone [44,45], polycarbonate [46], polyarylate [47], etc. This behavior could be attributed to the presence of H-bonding in PBI that brings chains closer, resulting in efficient chain packing. PBI–BuI and PBI–HFA exhibited two amorphous peaks, indicating that there could be two different types of predominant chain packing. A peak corresponding to the lower d_{sp} of 4.05 Å could be dominated by H-bonded region, while other peak at higher d_{sp} indicated looser chain packing dominated by bulky substitution (4.69 Å in case of PBI–BuI and 5.37 Å in case of PBI–HFA). PBI-T, PBI–BrT, PBI–DBrT and PBI–2,6Py exhibited higher chain packing density (lower d_{sp}) than that for PBI-I.

Though undoped membranes were amorphous in nature, after doping PBI-I, PBI–BuI and PBI–HFA with H_3PO_4, some crystallinity was induced in earlier two cases (Fig. 3). The appearance of crystallinity after acid doping was reported by Sannigrahi et al. for H_3PO_4-doped PBI-I [48]. PBI–HFA remained completely amorphous, probably due to lower doping level than the other two cases (given in Section 3.2.5).

3.2.2. Density and free volume

Density (ρ) measurement of the dry PBI films was performed by floatation method. Since present PBIs sorb considerable amount of water (Table 4), use of aqueous solutions for density measurement would have led to erroneous results. Thus, organic solvents that have appropriate density and do not get sorbed in PBI were selected for the density measurement. To determine solvent sorption in PBI, a film of ~100 μm thickness was dipped in these solvents for varying time. Iodomethane ($\rho = 2.275$ g/cm^3), tetrachloroethane ($\rho = 1.623$ g/cm^3) and cyclohexanone ($\rho = 0.9465$ g/cm^3) showed negligible sorption in all present PBIs (<1.5% w/w) for 2 h dip time and at 35 °C. This duration is sufficiently higher than the time required for the density measurement. The amount of solvent sorbed did not increase considerably even after 24 h dipping, except for iodomethane in PBI–DBrT (2.34%) and for TCE in PBI–HFA (13%). Initially the density of PBI-I was determined and compared with the literature data. The density in the present investigation was found to be 1.331 g/cm^3; while literature values are 1.3 g/cm^3 [49], 1.34 g/cm^3 [5] and 1.269 g/cm^3 [6]. In view of good agreement of measured density with the literature data, present method of the density estimation was extended for the density determination of other PBIs. Density of the halogenated PBIs (PBI–BrT/DBrT/HF) was higher than that of non-halogenated PBIs (PBI-I/T/2,6Py) (Table 3). Similar behavior can be seen in cases of other families of polymers such as polycarbonate [46], polyarylate [50], polysulfone [45], etc.

Measured density was used to estimate fractional free volume (v_f) and solubility parameter (δ) using the group additivity method

[35]. The results are given in Table 3. It was found that PBI–HFA exhibited the highest v_f among the series. Incorporation of *tert*-butyl group in PBI–BuI also led to an increase in v_f, indicating loose chain packing in comparison to the base case of PBI-I. These results are in agreement with the d_{sp} by WAXD, as discussed above. Incorporation of *tert*-butyl group or hexafluoroisopropylidene linkage in the main chain is known to render loose chain packing in cases of other polymers like polycarbonate [46], polysulfone [45], polyarylate [47,50], polyimide [51], etc. It is interesting to note that PBI-T (1,4-substitution on the acid moiety) exhibited slightly lower d_{sp} as well as v_f than that of PBI-I (1,3-substitution). On the contrary, in case of other aromatic polymers like polyarylates [52] or polyimides [51,53], it is known that polymer with 1,3-substitution leads to better chain packing than that of its isomer possessing 1,4-substitution. Incorporation of hexafluoroisopropylidene group (PBI–HFA) and *tert*-butyl group (PBI–BuI) in polymer backbone led to the lowering in solubility parameter (δ); while, incorporation of bromine (PBI–BrT and PBI–DBrT) and additional N (PBI–2,6Py) increased the v_f and δ in comparison to unsubstituted cases of PBI-I and PBI-T (Table 3).

3.2.3. *Thermal stability*

The thermogravimetric analysis (Fig. 4) revealed that all these PBIs exhibited initial loss below ~190 °C, attributable to the absorbed water [54]. The temperature at which this loss was completed (T_{wl}) is given in Table 3. It could be seen that for PBIs with higher free volume (PBI–BuI and PBI–HFA), this temperature was lower than that for other polybenzimidazoles. This could be attributable to the looser chain packing (higher v_f and d_{sp} in the series), which would ease the diffusion of water molecules from the bulk. In case of PBI–2,6Py, this temperature was highest among the series. This could be attributed to the combined effect of tighter chain packing (lower v_f) and the presence of additional nitrogen on the acid moiety, capable of providing additional H-bonding site to hold water molecules. PBI-I, PBI-T and PBI–2,6Py exhibited excellent thermal stability (≥600 °C, Table 3). High thermal stability associated with PBI was earlier ascribed to the aromatic rigid structure in the backbone [1,20,21] and could also be due to intermolecular H-bonding. This intermolecular H-bonding can be anticipated to be weaker in the case of PBI–BuI and PBI–HFA, as also indicated by their higher fractional free volume than that of other PBIs. Presence of the thermally labile group (–CF_3 or *tert*-butyl) and weaker H-bonding in these cases could be responsible for their observed lower thermal stability than that of PBI-I, PBI-T and PBI–2,6Py. Presence of *tert*-butyl group is known to lower the thermal stability [55]. Bromine containing PBI (PBI–BrT and PBI–DBrT) exhibited considerably lower degradation temperature than that of other PBIs.

3.2.4. *Water sorption*

Sorption of H_2O, H_3PO_4 and H_2SO_4 in present PBIs was examined in view of their applicability as a proton exchange membrane material. The vacuum dried PBI membranes were immersed in water for 3 days at ambient temperature and amount of water sorbed is determined gravimetrically. The maximum amount of water sorbed in different undoped PBIs was from 1.8 to 3.6 mol/RU (Table 4). These values are between the two limits as suggested by Brooks et al. [42]. According to this model, the hydrogen bonding of H_2O with PBI can occur in two ways. The first possibility would occur if two water molecules were attached to each imidazole ring, so that one water molecule could act as a proton acceptor and the other as a proton donor. This would allow a maximum of four H_2O molecules to be attached to each polymer repeat unit. The second possibility involves one water molecule attached to two neighboring imidazole rings from adjacent polymer chains. In this case the water molecule would act as both, proton acceptor as well as donor, which would allow a maximum of two H_2O molecules per polymer repeat unit.

3.2.5. *Acid sorption*

Initially, the time required for obtaining maximum possible acid sorption was determined using PBI-I membrane of ~40 μm thickness (Fig. 5) with the maximum possible acid concentration (16.2 M in case of H_3PO_4 and 12 M in case of H_2SO_4). It was found that the dip time required for achieving maximum acid sorption was 16 h with H_3PO_4 and 8 h with H_2SO_4 solution (Fig. 5). The literature reports this time to be as high as 50 h for H_3PO_4 and 5 h for H_2SO_4 solution [43,56]. The difference in thickness of the membrane used for this analysis could be a probable reason for this deviation.

The acid sorption at varying doping bath concentration was also investigated. Initially, sorption of both the acids (H_3PO_4 and H_2SO_4) was investigated at lower bath concentrations with shorter intervals (Fig. 6). It was found that the uptake was initially rapid up to 0.6 M H_3PO_4 and up to 0.2 M H_2SO_4, after which, the rate of increase is almost constant as indicated by the straight line nature of the graph beyond these bath concentrations. It could also be seen that uptake of acid by PBI was initially rapid in case of H_2SO_4 than that of H_3PO_4. This could be due to the difference in the acidity of H_3PO_4 and H_2SO_4. Since H_2SO_4 ($Ka_1 = 1 \times 10^2$) [57] is stronger acid than H_3PO_4 ($Ka_1 = 6.9 \times 10^{-3}$) [57], the rapid acid–base neutralization with PBI in former case may be responsible for this behavior.

The acid uptake by different PBIs using higher bath concentrations of H_3PO_4 and H_2SO_4 is given in Fig. 7. PBI–DBrT and PBI–BrT were found to dissolve in 16.2 M H_3PO_4, thus their doping characteristics were determined till 14.3 M H_3PO_4. Similarly, beyond 12 M of H_2SO_4, all PBI membranes were found to be soluble. The doping analysis with H_2SO_4 was restricted for PBI-I, PBI–BuI, PBI–HFA and PBI–2,6Py. A steady increase in H_3PO_4 doping was seen till 12 M concentration (Fig. 7a) and H_2SO_4 doping till ~11 M H_2SO_4 (Fig. 7b). Beyond these bath concentrations, two acids behaved differently. The H_3PO_4 doping showed an abrupt increase in doping level, while H_2SO_4 doping declined beyond these concentrations of doping bath. This could be correlated to the state of the polymer at higher bath concentrations. In the case of H_2SO_4, beyond 11 M concentration, PBI films tend to dissolve, showing slight decrease in acid uptake (due to some weight loss of PBI). On the contrary, PBI films were swollen considerably in H_3PO_4 beyond >12 M concentration. Li et al. [7,43] observed similar trend for H_3PO_4 doping in PBI-I in the concentration range 2–11 M and then the rapid increase in doping above 13 M H_3PO_4. Such sudden increase in acid uptake above 12–13 M H_3PO_4 could be correlated to the large swelling of the membrane matrix (which did not dissolve) at such higher doping bath concentration. For example, in 16.2 M H_3PO_4 concentration, an increase in length of PBI-I membrane was ~35% in comparison to undoped dry membrane, which after vacuum drying at 100 °C for a week was 20–22% for different samples, due to water loss. The wet membranes were highly flexible, swollen, stretchable and rubbery in nature.

It was found that for a particular PBI, doping of H_3PO_4 was higher than that of H_2SO_4 at the same doping bath concentration. This could be due to the tribasic nature of H_3PO_4, which can extend its H-bonding to more number of molecules, than dibasic H_2SO_4 could do, and thus can hold more number of acids surrounding it. The highest amount of doping in each PBI observed from Fig. 7 is compiled in Table 4, along with highest water sorption capacity. The amount of water sorbed as a function of acid bath concentration is plotted in Fig. 8. It could be seen that this amount of water sorbed along with the acid in any PBI is higher than water sorbed in only PBI (without acid), as given in Table 4. This could be explained on the basis of H-bonding of water with PBI as well as with acid present in the swollen state. Moreover, in the presence of acid, the swollen state of PBI membrane could also be responsible for this higher water uptake.

It can be seen from Table 4 that PBI–BuI, PBI–DBrT and PBI–2,6Py exhibited higher H_3PO_4 uptake of 20, 20.1 and 18.3 mol/RU, respectively; while PBI-T and PBI–HFA exhibited the lower uptake of 10.4 and 9 mol/RU, respectively than that of PBI-I. One of the factors responsible for this can be the swelling ability of these polymers in doping bath, as quantified by the summation of H_3PO_4 uptake and water uptake along with H_3PO_4, as given in Table 4. It becomes clear from Fig. 9 that as the swelling ability of the PBI increases, the acid uptake also increases. PBI–2,6Py and PBI–BuI showed the highest swelling, while PBI–HFA showed the lowest swelling. Better tendency to form H-bonding of PBI–BuI on the basis of its higher N–H group density (percent of molar mass of N–H group per repeat unit, which is 8.24%) could also be responsible for its higher acid uptake than that for PBI–HFA (N–H group density of 5.62%). PBI–DBrT and PBI–BrT were found to be soluble in H_3PO_4 at 16.2 M concentration. Presence of a single bromo group (PBI–BrT) imparting polarity to this PBI was enough to render solubility in 16.2 M H_3PO_4; while presence of two bromine atoms in PBI–DBrT not only imparted polarity, but also led to a looser chain packing. The increased polarity by two bromo groups could be responsible for its higher H_3PO_4 uptake in comparison to the base case of PBI-I, before it could get actually dissolved in the higher concentration of H_3PO_4 (16.2 M). This also can be evident from Fig. 7a, where the doping level at a certain H_3PO_4 bath concentration was higher for PBI–DBrT than for other PBIs.

Highest H_2SO_4 uptake in PBIs investigated was from 3.39 to 3.81 mol/RU (Table 4). Since H_2SO_4 is dibasic in nature and its highest uptake in a particular PBI being <4 mol/RU, doping behavior of H_2SO_4 can be explained based on Brook's model, as given in Section 3.2.4. The maximum amount of water sorption in virgin PBI varied from 1.8 to 3.6 mol/RU, while the sorption of H_2SO_4 varied in a shorter range. This could be attributed to the strong acidity of H_2SO_4, wherein each molecule would prefer to release first proton to each 'N' of the imidazole, following 'first' possibility suggested by Brooks et al. (Section 3.2.4) [42]. In H_2SO_4 doping bath, acid–base complex formation with 'N' of imidazole would take place by releasing first proton of H_2SO_4. One molecule releasing two protons to two neighboring 'N' of imidazole rings is unlikely, since release of second proton ($Ka_1 = 1 \times 10^2$, $Ka_2 = 1 \times 10^{-2}$) is unlikely in view of availability of H_2SO_4 in the doping bath. In comparison to H_3PO_4, uptake of H_2SO_4 is lower in a particular PBI. This could be due to the higher acidity of H_2SO_4 (unable to hold another H_2SO_4 molecule due to H-bonding in its neighborhood) and also due to its dibasic nature, vis-à-vis tribasic nature of H_3PO_4.

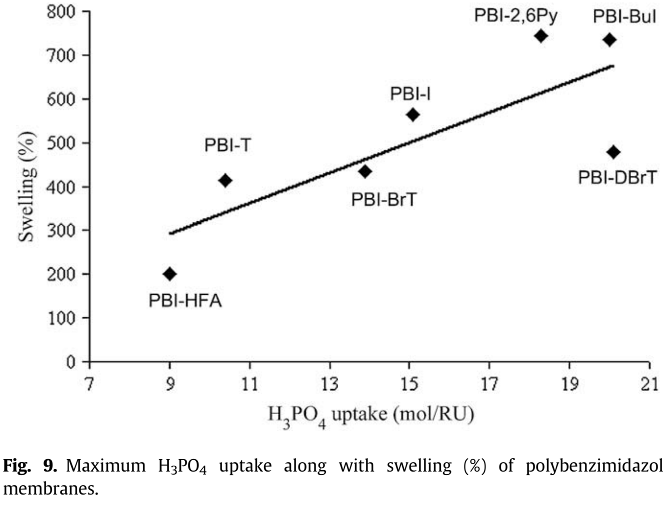

Fig. 9. Maximum H_3PO_4 uptake along with swelling (%) of polybenzimidazole membranes.

3.2.6. Physical state of H_3PO_4-doped PBI-I

In view of swelling behavior of present PBIs in H_3PO_4 and their applicability as PEM for fuel cell, it would have been advantageous to determine the T_g of H_3PO_4-doped PBIs. It could not be attempted since it is known that beyond 150 °C, H_3PO_4 shows continuous weight loss due to dehydration to form pyrophosphoric acid and metaphosphoric acid [54]. Increase of the temperature during DSC scan of the acid doped PBI would loose water, leading to change in the original composition of the sample. Thus, determination of T_g of the acid doped PBI by DSC would not offer realistic results. Alternatively, we determined the volume of dry H_3PO_4-doped PBI membrane samples, with varying doping content, which could be correlated to T_g. The volume of dry PBI-I samples with increasing amount of H_3PO_4 was determined by He gas expansion method [36] as described in Section 2.6 under isothermal condition (35 °C). The variation in inverse of estimated density ($1/\rho$) of H_3PO_4-doped PBI-I with the varying level of H_3PO_4 doping (mol/RU) is shown in Fig. 10. It could be seen that up to $\sim$6 mol/RU uptake of H_3PO_4, there is an abrupt decrease in $1/\rho$ of the doped membrane, beyond which, slope of the curve becomes almost linear. This abrupt decrease in $1/\rho$ could be correlated to the change in the physical state of PBI-I, which can be assumed as the transformation of glassy state to the rubbery state. Beyond doping level of $\sim$10 mol/RU, slope of the curve became almost constant. This can be correlated to attaining rubbery state of PBI after this doping level. In other words, it could be speculated that at the temperature of this analysis (35 °C), PBI-I could be in rubbery state beyond doping level of $\sim$10 mol/RU. This information may be crucial for applicability of PBI-I as the proton exchange membrane material. The dry doped PBI-I membranes with lower acid uptake ($\leq$6 mol/RU) were tough films; while those doped with higher uptake were more flexible in nature. More investigations may be required to confirm this speculation.

3.3. Gas permeability

The gas permeability coefficients and selectivities (the ratio of pure gas permeability) for H_2 and O_2 for these PBIs were

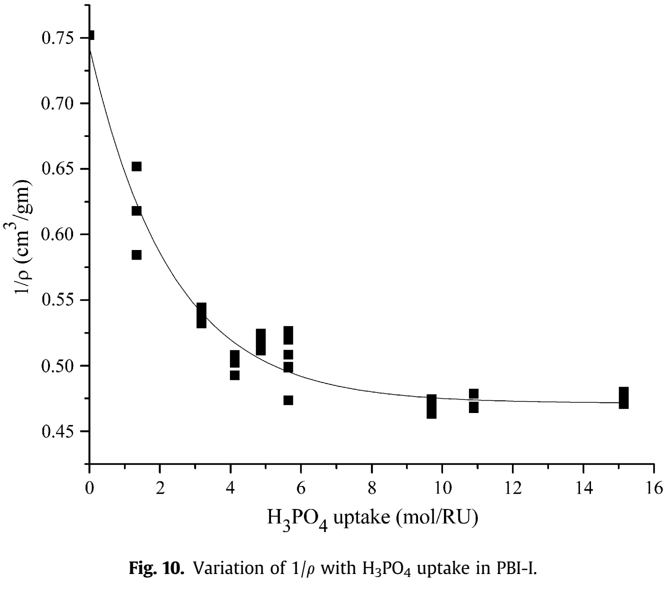

Fig. 10. Variation of $1/\rho$ with H_3PO_4 uptake in PBI-I.

investigated in view of their applicability as PEM or gas separation membrane material (Table 5). One of the criteria for a polymer to be applicable as PEM material is that it should have low permeability for the two gases, H_2 and O_2 [48,58]. Three PBI membranes were doped and evaluated for gas permeability. The conventional PBI (PBI-I), and two PBIs with bulky substitutions (PBI–BuI and PBI–HFA) were chosen for this purpose. It was seen that permeability of H_2 and O_2 after doping with H_3PO_4 was much lower in comparison to Nafion-117 membrane (widely demonstrated membrane for PEMFC application), measured at 25 °C [58]. Thus, they could be used as PEM materials.

Permeability investigations of undoped PBIs showed an interesting behavior. It was observed that PBI-T exhibited the lowest permeability, while PBI–HFA exhibited the highest. The permeability difference was 76-fold for H_2 and 150-fold for O_2. The low permeability of PBI-I was earlier attributed to the presence of H-bonding [9–11]. The permeability increase was in the order: PBI-T < PBI–BrT < PBI-I < PBI–2,6Py < PBI–DBrT < PBI–BuI < PBI–HFA; The $\alpha(H_2/O_2)$ selectivity followed almost a reverse order, except for PBI–BrT and PBI-T. PBI–BrT showed the highest selectivity of 60 in the series, following a general trade-off relationship of permeation properties (structural modifications in a polymer backbone leading to the lowering in permeability increase selectivity and vice versa). As expected, the bulky *tert*-butyl group in the case of PBI–BuI and hexafluoroisopropylidene group in the case of PBI–HFA leading to the inefficient packing due to the bulk of these groups (higher v_f) were responsible for their higher permeabilities. PBI–HFA showed 19 and 40 times higher permeability for H_2 and O_2, respectively, than that of PBI-I. The respective increase in permeability of PBI–BuI was 16.9 and 28 times. Though similar behavior of increase in permeability by substitution of *tert*-butyl and hexafluoroisopropylidene group is well known in other families of polymers, such as polyarylate [47,50], polyimide [51], polycarbonate [46], etc.; similar increase in permeability was from 3.2 to 4.5 times, in comparison to the respective base unsubstituted polymer, selectivity being considerably lower than the PBI investigated in this work. A larger increase in permeability for PBI family by bulky group substitution could be explained on the basis of initial lower permeability of PBI-I. The presence of H-bonding reduces the available free volume and thus permeability (which is much lesser than the conventional polymers like PC, PSF, etc.). The substitution by bulky *tert*-butyl and hexafluoroisopropylidene groups disrupts this H-bonding to a certain extent, as also supported by the appearance of two peaks in WAXD spectra and an increase in fractional free volume. On the other hand, higher selectivity can be explained based on the higher rigidity of PBI. Higher T_g of PBI-I (430 °C) allows better penetrant discriminating ability (and thus high selectivity) than shown by common polymers like PC (T_g of 150 °C) or PSF (T_g of 186 °C).

PBI-T (1,4-substitution on acid moiety) exhibited lower permeability coefficient and higher selectivity in comparison with PBI-I (1,3-substitution in acid), which is attributable to its higher packing density as evident from its lower *d*-spacing and v_f values. This trend in permeability and selectivity for these isomeric PBIs is reverse than the trend observed in cases of other polymers with 1,3- and 1,4-substituted isomers. For example, the isophthalic acid based polyarylates have less permeability and higher selectivity than the terephthalic acid based polyarylates, derived from same bisphenol [52]. In case of polyimides also, 1,3-substituted polymer exhibited lower permeability and higher selectivity than its 1,4-substituted analogue [51,53].

The substitution of bromine atom in PBI–BrT elevated its v_f and thus gas permeability, in comparison to the unsubstituted PBI-T case. An increase in permeability by dibromo substitution in PBI–DBrT was more than the case of monobromo substitution in PBI–BrT, which could be correlated to further increase in v_f by the dibromo substitution.

It would also be worth to compare the permeability and selectivity of these PBIs with widely investigated polymer materials for gas permeability like polysulfone and polyarylate. It can be seen from Table 5 that these PBIs (except PBI–BuI and PBI–HFA) have lower permeability but substantially higher selectivity than these properties for polyarylate or polysulfone. Efforts of structural modification in PBI towards improving permeability, as in PBI–BuI and PBI–HFA elevated the H_2 permeability, which is closer to polyarylate or polysulfone, while O_2 permeability still remained lower. This led to 2–3 times higher selectivity for PBI–HFA and PBI–BuI than that for polyarylate or polysulfone. This behavior can be attributed to the rigid chain backbone of PBI (higher T_g) than other polymer families. In other words, though the structural modifications in these PBIs (PBI–HFA and PBI–BuI) increased permeability, it retained its capability of better discriminating between different penetrants and thus can serve as better gas separation membrane materials.

4. Conclusions

All the PBIs derived from 3,3′-diaminobenzidine and various substituted aromatic dicarboxylic acids were amorphous in nature and exhibited high degradation temperature (>400 °C). An introduction of *tert*-butyl group in PBI–BuI, hexafluoroisopropylidene group in PBI–HFA, bromine in PBI–BrT and PBI–DBrT enhanced the solvent solubility of these PBIs. The doping level of H_3PO_4 in PBIs was higher than that of H_2SO_4 at the same doping bath concentration due to tribasic nature of H_3PO_4. The higher acid uptake of PBI–BuI (20 mol/RU) and PBI–DBrT (20.1 mol/RU) than that of PBI-I (15.1 mol/RU) suggested potential for their use as the proton exchange membrane material. The high H_3PO_4 uptake was related to the swelling ability of the PBI. Higher N–H group density for PBI–BuI and polarity of bromo group in PBI–DBrT elevated doping level of H_3PO_4 for these PBIs. He gas expansion method was used to determine the volume and thus the density of dry H_3PO_4-doped PBI-I samples. This analysis could lead to a speculation that at 35 °C, H_3PO_4-doped PBI-I could be glassy below the acid uptake of 6 mol/RU, while it possesses rubbery nature beyond uptake of 10 mol/RU. The addition of bulk in case of PBI–BuI and PBI–HFA increased permeability by 16.9–40 times than that of unsubstituted PBI. Though the selectivities in these PBIs were reduced than the base case of PBI-I, they were 2–3 times higher than the conventional gas separation materials like polycarbonate or polysulphone. The isomeric PBI-I and PBI-T showed unusual variation in their v_f and thus gas permeability in comparison to other isomeric polymers like polyimide and polyarylate. The high gas selectivity of these PBIs combined with high thermal stability suggested that they could be good candidates for gas separation application.

Acknowledgements

Financial support from NMITLI program (Grant No. 5/258/35/2004-NMITLI) is duly acknowledged.

References

[1] Vogel H, Marvel CS. J Polym Sci 1961;50(154):511–39.
[2] Li Q, He R, Jensen JO, Bjerrum NJ. Chem Mater 2003;15:4896–915.
[3] Li Q, He R, Jensen JO, Bjerrum NJ. Fuel Cell 2004;4(3):147–59.
[4] Wainright JS, Wang J-T, Weng D, Savinell RF, Litt M. J Electrochem Soc 1995;142(7):121–3.
[5] Mecerreyes D, Grande H, Miguel O, Ochoteco E, Marcilla R, Cantero I. Chem Mater 2004;16:604–7.

[6] Foldes E, Fekete E, Karasz FE, Pukanszky B. Polymer 2000;41:975–83.
[7] Li Q, Hjuler HA, Bjerrum NJ. J Appl Electrochem 2001;31:773–9.
[8] Mak CM, Yuen CWM, Ku SK, Tao XM. Textile Asia 2002;33(2):39–41.
[9] Pesiri DR, Jorgensen B, Dye RC. J Membr Sci 2003;218:11–8.
[10] Kumbharkar SC, Karadkar PB, Kharul UK. J Membr Sci 2006;286:161–9.
[11] Jorgensen BS, Young JS, Espinoza BF. U.S. Patent 0261616; 2004.
[12] Belohlav LR. Angew Makromol Chem 1974;40(1):465–83.
[13] Strauss EL. Polym Eng Sci 1966;6(1):24–9.
[14] Bouchet R, Rosini S, Vitter G, Siebert E. Sens Actuators B 2001;76:610–6.
[15] Zaidi SMJ. Electrochim Acta 2005;50:4771–7.
[16] Chung TS, Guo WF, Liu Y. J Membr Sci 2006;271:221–31.
[17] Sun H, Mark JE, Tan SC, Venkatasubramanian N, Houtz MD, Arnold FE, et al. Polymer 2005;46:6623–32.
[18] Leinonen SM, Sherrington DC. J Chem Res (S) 1999:572–3.
[19] Kim JS, Reneker DH. Polym Eng Sci 1999;39(5):849–54.
[20] Gerber AH. J Polym Sci Polym Chem Ed 1973;11(7):1703–19.
[21] Vogel H, Marvel CS. J Polym Sci Part A Gen Pap 1963;1(5):1531–41.
[22] Bhowmik S, Bonin HW, Bui VT, Weir RD. J Appl Polym Sci 2006;102:1959–67.
[23] Lyoo WS, Choi JH, Han SS, Yoon WS, Park MS, Ji BC, et al. J Appl Polym Sci 2000;78(2):438–45.
[24] Tsur Y, Levine HH, Levy M. J Polym Sci Polym Chem Ed 1974;12(7):1515–29.
[25] Iwakura Y, Uno K, Imai Y. J Polym Sci Part A Gen Pap 1964;2(6):2605–15.
[26] Scariah KJ, Krishnamurthy VN, Rao KVC. J Polym Sci Part A Polym Chem 1987;25:2675–87.
[27] Korshak VV, Teplyakov MM, Fedorova RD. J Polym Sci Part A-1 Polym Chem 1971;9(4):1027–43.
[28] Srinivasan PR, Mahadevan V, Srinivasan M. J Polym Sci Polym Chem Ed 1982;20(11):3095–105.
[29] Foster RT, Marvel CS. J Polym Sci Part A Gen Pap 1965;3(2):417–21.
[30] Lakshmi Narayan TV, Marvel CS. J Polym Sci Part A-1 Polym Chem 1967;5(5):1113–8.
[31] Nakajima T, Marvel CS. J Polym Sci Part A-1 Polym Chem 1969;7(5):1295–8.
[32] Mulvaney JE, Marvel CS. J Polym Sci 1961;50(154):541–7.
[33] Kovacs HN, Delman AD, Simms BB. J Polym Sci Part A-1 Polym Chem 1968;6(8):2103–15.
[34] Saegusa Y, Horikiri M, Nakurmura S. Macromol Chem Phys 1997;198(2):619–25.
[35] Van Krevelen DW. Properties of polymers: correlation with chemical structure. Amsterdam: Elsevier Science; 1997 [chapter 7].
[36] Rutherford SW, Kurtz RE, Smith MG, Honnell KG, Coons JE. J Membr Sci 2005;263:57–65.
[37] Karadkar PB, Kharul UK, Bhole YS, Badhe YP, Tambe SS, Kulkarni BD. J Membr Sci 2007;303:244–51.
[38] Stern SA, Shah VM, Hardy BJ. J Polym Sci Part B Polym Phys 1987;25:1263–98.
[39] Choi EJ, Hill DJT, Kim KY, O'Donnell JH, Pomery PJ. Polymer 1997;38(14):3669–76.
[40] Musto P, Karasz FE, MacKnight WJ. Polymer 1989;30(6):1012–21.
[41] Musto P, Karasz FE, MacKnight WJ. Polymer 1993;34(14):2934–45.
[42] Brooks NW, Duckett RA, Rose J, Ward IM. Polymer 1993;34(19):4038–42.
[43] Li Q, He R, Berg RW, Hjuler HA, Bjerrum NJ. Solid State Ionics 2004;168:177–85.
[44] McHattie JS, Koros WJ, Paul DR. Polymer 1991;32(5):840–50.
[45] McHattie JS, Koros WJ, Paul DR. Polymer 1992;33(8):1701–11.
[46] Hellums MW, Koros WJ, Husk GR, Paul DR. J Membr Sci 1989;46:93–112.
[47] Pixton MR, Paul DR. Macromolecules 1995;28:8277–86.
[48] Sannigrahi A, Arunbabu D, Jana T. Macromol Rapid Commun 2006;27:1962–7.
[49] Tarasevich MR, Karichev ZR, Bogdanovskaya VA, Kuznetsova LN, Efremov BN, Kapustin AV. Russ J Electrochem 2004;40(6):653–6.
[50] Kharul UK, Kulkarni SS. Bull Mater Sci 1994;17(6):1071–7.
[51] Coleman MR, Koros WJ. J Membr Sci 1990;50:285–97.
[52] Pessan LA, Koros WJ. J Polym Sci Part B Polym Phys 1993;31:1245–52.
[53] Coleman MR, Koros WJ. J Polym Sci Part B Polym Phys 1994;32:1915–26.
[54] Asensio JA, Borros S, Gomez-Romero P. J Polym Sci Part A Polym Chem 2002;40:3703–10.
[55] Schild HG, Kolb ES, Mehta PG, Ford M, Gaudiana RA. Polymer 1994;35(6):1222–8.
[56] Glipa X, Bonnet B, Mula B, Jones DJ, Roziere J. J Mater Chem 1999;9:3045–9.
[57] Atkins P, de Paula J. Atkins' physical chemistry. 7th ed. Oxford: Oxford University Press; 2002.
[58] He R, Li Q, Bach A, Jensen JO, Bjerrum NJ. J Membr Sci 2006;277:38–45.